Performance Evaluation of Doubly Fed Induction Generator Based Wind Turbine

3 authors:

Dahiru Musbahu
Federal University of Technology Minna
3 PUBLICATIONS **1** CITATION

SEE PROFILE

Gbenga Olarinoye
Ahmadu Bello University
31 PUBLICATIONS **66** CITATIONS

SEE PROFILE

Adamu Saidu Abubakar
Ahmadu Bello University
47 PUBLICATIONS **182** CITATIONS

SEE PROFILE

Performance Evaluation of Doubly Fed Induction Generator Based Wind Turbine

D. Musbahu[1], G.A. Olarinoye[2] and A.S. Abubakar[3]

[1](Department of Electrical Engineering, Ahmadu Bello University, Zaria – Nigeria).
[2](Department of Electrical Engineering, Ahmadu Bello University, Zaria – Nigeria).
[3] (Department of Electrical Engineering, Ahmadu Bello University, Zaria – Nigeria).

[1]dahirumisbahu@gmail.com, [2]oyeguzeh@yahoo.com, [3]abubakaras@abu.edu.ng

Abstract: **This paper is an analysis of a MATLAB/Simulink model of the Doubly-fed Induction Generation (DFIG)-based wind turbine and its evaluation. It covers the aero dynamic model, rotor and grid side control models and the model of the DFIG. Many authors have presented similar models but this paper develops a Simulink model of the DFIG by using the analytical equations of the DFIG instead of the single DFIG block contained in the Simscape library of the Simulink software. An adequate description of the solution of this analytical model is provided. The control strategy was also implemented using appropriate function blocks in the Simulink environment and some MATLAB scripts. This work evaluates the performances of rotor speed, DC link voltage, rotor active and reactive power and the grid current. The response of rotor speed after wind speed changed from 8 m/s to 10 m/s is provided. The DC link voltage is controlled to a constant value of 1150 V to keep rotor power constant while the reactive power of the rotor is regulated at 0 VAR thereby ensuring that no reactive power is exchanged with the grid. A rise in rotor active power with less torque was observed with the step change in speed. The grid current waveform was observed to be a 50Hz, 3-phase sinusoidal current with amplitude of 500 A Peak to Peak (*pk-pk*).**

Keywords: Doubly Fed Induction Generator (DFIG); Grid Side Converter (GSC); Vector Control; Wind Turbine, Rotor side Converter (RSC);

I.   INTRODUCTION

Conventional energy sources such as oil and coal etc. are depleting and causing harm to the environment. This has led to increasing interest to utilize safer sources of energy such as wind, fuel cell, bio-thermal and solar energy. Of all these sources, wind energy is the fastest growing energy source because it is economically viable and pollution free [1]. Wind energy is obtained with wind turbines. DFIGs are often coupled to wind turbines and are used to generate large amounts of power. The rotating speed of the DFIG can be changed in proportion to the changing wind speed and this makes it necessary to optimize the power extracted from the wind [2]. The DFIG based wind turbine also provides flexible control of active and reactive power exchange with the grid and they have high efficiency at considerably low cost. A lot research has been carried out on wind energy conversion systems. Reference [3] developed an integrated mechanical and electrical DFIG Wind Turbine Model. A typical 1.5MW DFIG-based wind turbine was modeled using MATLB/Simulink and FAST. In [4], a Model of the DFIG-based variable speed wind turbine was presented, in which steady state operation and control of DFIG was investigated. The performance of Indirect Matrix Converter with improved control of the doubly fed Induction Machine was studied in [5]. A wind energy conversion system equipped with the DFIG is shown in Figure 1. The generator is a wound rotor asynchronous machine. Variable speed operation is obtained by injecting a variable voltage into the rotor at slip frequency. Voltage is injected from the output of the back-to-back AC/DC voltage source converters (VSC), equipped with passive filters. A vector control strategy provides the control of DFIG based on PI controllers [6]. The objective of this paper is to describe the solution of the analytical model of the DFIG based wind turbine and to evaluate and discuss the generator performances.
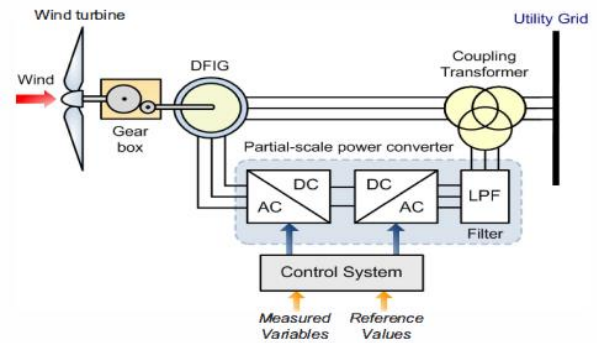

Figure 1. The DFIG wind turbine system

II. DFIG-BASED WIND TURBINE MODELING

The DIFIG-based wind turbine configuration includes the mechanical parts (i.e. the aerodynamic system with rotor blades and the gear box) and the electrical parts (i.e. the DFIG and the back-back converter set)

A. The Wind Turbine (WT) Model

The mechanical power extracted from the wind by the wind turbine is given as follows [7]

$$P_m = \frac{1}{2}\rho\pi R^2 C_p(\lambda,\beta)V_w^3 \qquad (1)$$

where ρ is the air density in kg/m^3, R is the radius of turbine blade, V_w is the wind speed in m/s, C_p is the power coefficient and β is the pitch angle. The tip speed ratio λ is defined as the ratio of the angular rotor speed of the wind turbine to the linear wind speed at the tip of the blades and can be expressed as follow:

$$\lambda = \frac{w_r R}{V_w} \qquad (2)$$

w_r is the mechanical angular velocity of the rotor . The driving torque around the rotor shaft is given by the following equation [8];.

$$T_m = \frac{1}{2}\rho A R C_T V_w^2 \qquad (3)$$

where C_T is the torque coefficient given by;

$$C_T = \frac{C_p}{\lambda} \qquad (4)$$

The coefficient C_p is calculated based on variable speed wind turbine as follows:

$$\lambda_i = \frac{1}{\frac{1}{\lambda + 0.002\beta} - \frac{0.03}{\beta^3 + 1}} \qquad (5)$$

$$C_P(\lambda,\beta) = 0.73\left[\frac{151}{\lambda} - 0.58\lambda - 0.002\beta^{2.14} - 13.2\right]e^{\frac{184}{\lambda_i}} \qquad (6)$$

The aerodynamic model of the three-blade wind turbine model represented by equations (2) - (6) was implemented in the Simulink program. The torque coefficient C_t *vs* λ curve of Figure 2 obtained according to the model equations was implemented in the Simulink program to emulate a three-blade wind turbine. λ is a variable that ranges from 0.1 – 11.8. For a wind speed range of 0 – 15m/s, the power *vs* wind speed curve was plotted according to equation (1) and provided in Figure 3. It is a prediction of the

mechanical power obtainable from the DFIG for the representative wind speeds.
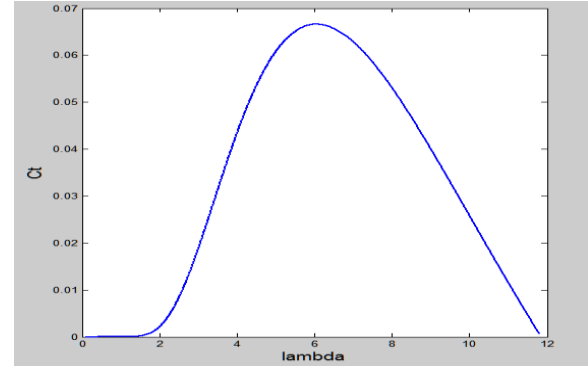

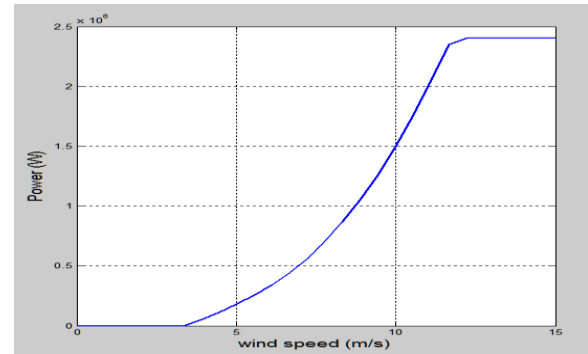Figure 2: Torque coefficient of the Turbine versus tip-speed ratio

Figure 3: Turbine output power versus wind speed

The reference electromagnetic torque is expressed as follows:

$$T = \frac{1}{2}\rho\pi R^5 \frac{(C_p)max}{(\lambda_{opt})^3}w_r^2 \qquad (7)$$

where, λ_{opt} is the tip speed ratio tuned to optimal value over different wind speeds. The electromagnetic torque reference can also be expressed as;

$$T = k_{opt}w_r^2 \qquad (8)$$

where w_r is rotor rotational speed obtained from the generator shaft.

$$k_{opt} = \frac{1}{2}\rho\pi R^5 \frac{(C_p)max}{(\lambda_{opt})^3}w_r^2 \qquad (9)$$

A basic MPPT strategy illustrated in Figure 4 was also implemented in Simulink. In this strategy, the rotor speed is fed back, squared and multiplied by optimum constant k_{opt} obtained from equation (9) in order to produce the torque reference working to its optimum speed value, and therefore power value, according to the wind speed that has been set.
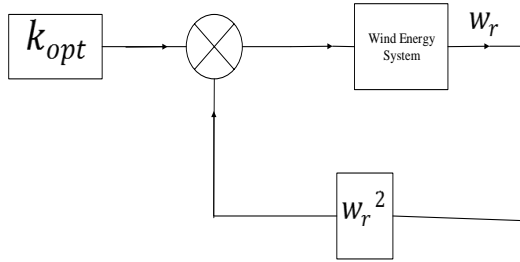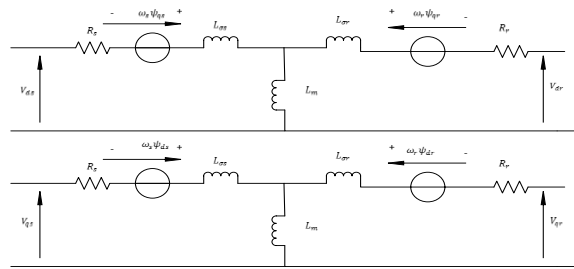
Figure 4: MPPT controller

The WT operates optimally to track maximum power from the wind.

B.   DFIG Modeling

The $d - q$ equivalent circuit diagram of the DFIG is shown in Figure 5 [8].

Figure 5: The d-q equivalent circuit of a DFIG

The stator and rotor $d - q$ voltage and flux equations are given by the following equations:

$$\begin{cases} V_{ds} = R_s i_{ds} + \dfrac{d\psi_{ds}}{dt} - jw_s\psi_{qs} \\ V_{qs} = R_s i_{qs} + \dfrac{d\psi_{qs}}{dt} + jw_s\psi_{ds} \end{cases} \tag{10}$$

$$\begin{cases} V_{dr} = R_r i_{dr} + \dfrac{d\psi_{dr}}{dt} - jw_r\psi_{qr} \\ V_{qr} = R_r i_{qr} + \dfrac{d\psi_{qr}}{dt} + jw_r\psi_{dr} \end{cases} \tag{11}$$

$$\begin{cases} \psi_{ds} = L_s i_{ds} + L_m i_{dr} \\ \psi_{qs} = L_s i_{qs} + L_m i_{qr} \end{cases} \tag{12}$$

$$\begin{cases} \psi_{dr} = L_r i_{dr} + L_m i_{ds} \\ \psi_{qs} = L_r i_{qr} + L_m i_{qr} \end{cases} \tag{13}$$

where R_s and R_r are the stator and rotor resistances, L_s and L_r are the stator and rotor inductance while L_m represents the mutual inductance. w_s is the synchronous (stator) frequency. Subscript s and r indicates the stator and rotor variables. In addition V_s, i_s and ψ_s represent the stator voltage, current and flux respectively and V_r, i_r and ψ_r represent the rotor voltages, current and flux vectors respectively.

The stator and rotor active and reactive power equations are given by the following expressions.

$$P_s = 1.5(V_{ds} i_{ds} + V_{ds} i_{ds}) \tag{14}$$

$$P_r = 1.5(V_{dr} i_{dr} + V_{dr} i_{dr}) \tag{15}$$

$$Q_s = 1.5(V_{qs} i_{ds} - V_{ds} i_{qs}) \tag{16}$$

$$Q_r = 1.5(V_{qr} i_{dr} - V_{dr} i_{qr}) \tag{17}$$

where P and Q denote active and reactive power respectively.

The DFIG Simulink program was derived by using the analytical model of equations (10) – (13). The state space representation of the model is obtainable from the analytical model and is given as follows;

$$\frac{d}{dt}\begin{bmatrix} \psi_{\alpha s} \\ \psi_{\beta s} \\ \psi'_{\alpha r} \\ \psi'_{\beta r} \end{bmatrix} = \begin{bmatrix} \dfrac{-R_s}{\sigma L_s} & 0 & \dfrac{R_s L_m}{\sigma L_s L_s} & 0 \\ 0 & \dfrac{-R_s}{\sigma L_s} & 0 & \dfrac{R_s L_m}{\sigma L_s L_s} \\ \dfrac{R_s L_m}{\sigma L_s L_s} & 0 & \dfrac{R_s}{\sigma L_s L_s} & -\omega_r \\ 0 & \dfrac{R_s L_m}{\sigma L_s L_s} & \omega_r & \dfrac{-R_r}{\sigma L_s} \end{bmatrix}\begin{bmatrix} \psi_{\alpha s} \\ \psi_{\beta s} \\ \psi'_{\alpha r} \\ \psi'_{\beta r} \end{bmatrix} + \begin{bmatrix} V_{\alpha s} \\ V_{\beta s} \\ V'_{\alpha r} \\ V'_{\beta r} \end{bmatrix} \tag{18}$$

$$\begin{bmatrix} i_{\alpha s} \\ i_{\beta s} \end{bmatrix} = \begin{bmatrix} \dfrac{-R_s}{\sigma L_s} & 0 & \dfrac{-L_m}{\sigma L_s L_s} & 0 \\ 0 & \dfrac{-R_s}{\sigma L_s} & 0 & \dfrac{-L_m}{\sigma L_s L_s} \end{bmatrix}\begin{bmatrix} \psi_{\alpha s} \\ \psi_{\beta s} \\ \psi'_{\alpha r} \\ \psi'_{\beta r} \end{bmatrix} \tag{19}$$

$$\lambda'_r = \frac{L_m}{L_s}\lambda_s + \sigma L_r i_r \tag{20}$$

The Simulink program was developed from the state space equations. The stator and rotor fluxes were chosen as the state variables. The advantage of this choice is that the equations are shorter and the expressions are simpler than the case in which stator and rotor currents are chosen as the state variables. In solving the state space model of the DFIG, the following steps were implemented in the Simulink program;

1. Matrix evaluation of equation (18) was performed.
2. The result was integrated to obtain the fluxes
3. Stator and rotor currents were calculated from the fluxes according to equations (19) and (20)

Stator voltages are inputs to the program while torque, speed, rotor angular position and rotor currents are the outputs of the model.

C.   DFIG Vector Control Technique

The decoupled control of the DFIG active and reactive power was achieved using a vector control technique. This technique is applied to the rotor side control and the grid side control.

        a.   Rotor Side Control

The rotor side converter (RSC) with the help of vector control ensures the control of stator active and reactive power using PI controllers through control of rotor direct and quadrature current components under stator flux orientation. Figure 6 illustrates the Simulink implementation of the RSC control.

        b.   Grid Side Control

Similarly, grid side converter (GSC) ensures the control of dc link voltage and reactive power exchange between the GSC and the grid. The space vector of the grid voltage is aligned with the d axis of the dq rotating reference frame. Figure 7 illustrates the Simulink implementation of the grid side converter control.

D.   PI Controller Design

The RSC and GSC each consists of two control loops (i.e. inner and outer control loops). The RSC inner control loop regulates the d-q rotor current component using a PI controller for each current component.

The controller designed for inner control loop was based on the d-q rotor voltage equation as follows:

$$V_{dr} = R_r i_{dr} + \sigma L_r \frac{d}{dt} i_{dr} - w_r \sigma L_r i_{qr} +$$
$$\frac{L_m}{L_s} \frac{d}{dt} |\overrightarrow{\Psi_s}| = V_{dr}{}^1 + V_{dr}{}^2 \tag{21}$$

$$V_{qr} = R_r i_{qr} + \sigma L_r \frac{d}{dt} i_{qr} + w_r \sigma L_r i_{dr} + \frac{L_m}{L_s} |\overrightarrow{\Psi_s}| =$$
$$V_{qr}{}^1 + V_{qr}{}^2 \tag{20}$$

Where; $V_{dr}{}^1$ and $V_{qr}{}^1$ are called current regulation parts and are given by;

$$V_{dr}{}^1 = R_r i_{dr} + \sigma L_r \frac{d}{dt} i_{dr} \tag{22}$$

$$V_{qr}{}^1 = R_r i_{qr} + \sigma L_r \frac{d}{dt} \tag{23}$$

For each current component the control loop diagram is as shown in Figure 8.

The transfer function of the rotor current control loops in the frequency domain is given as follows;

$$\frac{i_{dr}}{i_{dr}{}^*} = \frac{sK_p + K_i}{s^2(\sigma L_r) + s(R_r + K_p) + K_1} \tag{24}$$

$$\frac{i_{qr}}{i_{qr}{}^*} = \frac{sK_p + K_i}{s^2(\sigma L_r) + s(R_r + K_p) + K_1} \tag{25}$$

The rotor current control loop dynamics can be approximated by a second-order system dynamics. The denominator of equation (24) can be matched with the denominator of second-order system as follows.

$$s^2(\sigma L_r) + s(R_r + K_p) + K_1 = s^2 + 2\xi w_n s + w_n{}^2 \tag{26}$$

where w_n is the natural frequency in rad/s and ξ the damping ratio. By normalizing (26) and equating coefficients, the PI controller gains K_p and K_i were evaluated as follows:

$$s^2 + \left(\frac{R_r + K_p}{\sigma L_r}\right) s + \frac{K_i}{\sigma L_r} = s^2 + 2\xi w_n s + w_n{}^2 \tag{27}$$

$$\frac{R_r + K_p}{\sigma L_r} = 2\xi w_n \tag{28}$$

$$\frac{K_i}{\sigma L_r} = w_n{}^2 \tag{29}$$

Therefore,

$$\begin{cases} K_p = 2\xi w_n \sigma L_r - R_r \\ K_i = \sigma L_r w_n{}^2 \end{cases} \tag{30}$$

where L_r, R_r are the rotor inductance and rotor resistance. K_p, K_i are the proportional and integral controller gains. The system was chosen to be critically damped. The damping ratio and natural frequencies were chosen as follows;

$$w_n = \frac{\sigma L_r}{R_r} \qquad \xi = 1, \tag{31}$$

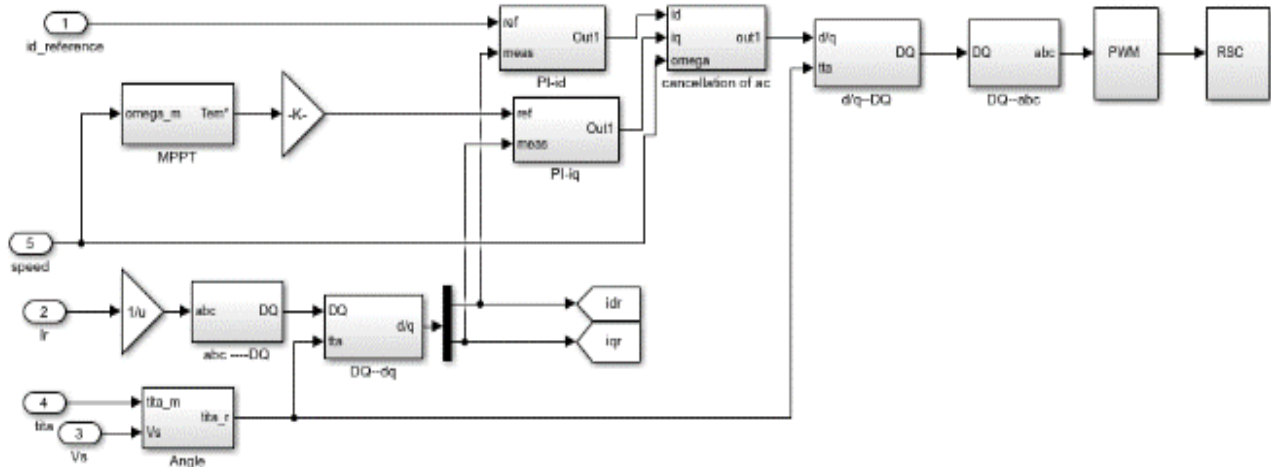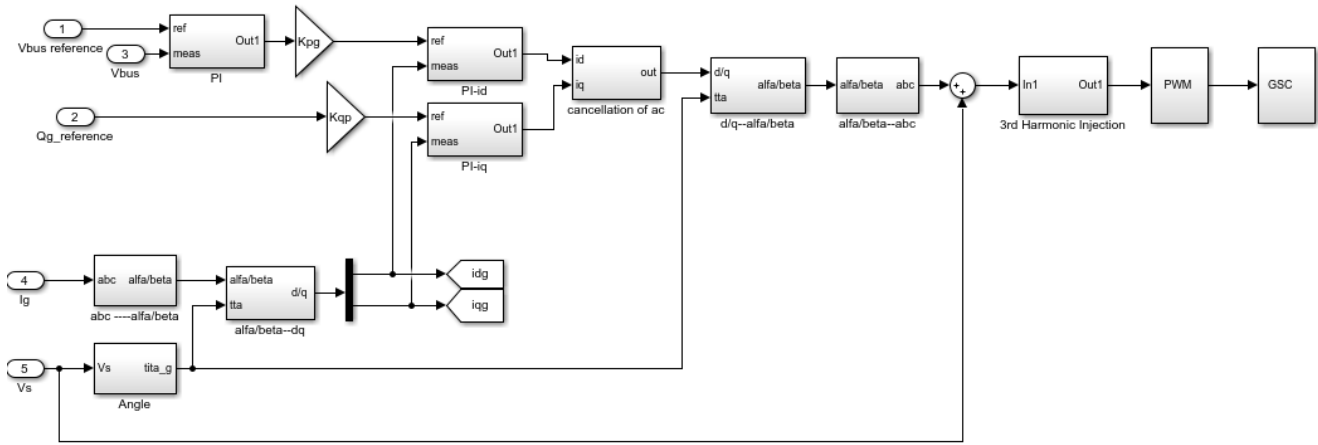

Figure 6 Structure of rotor side converter control

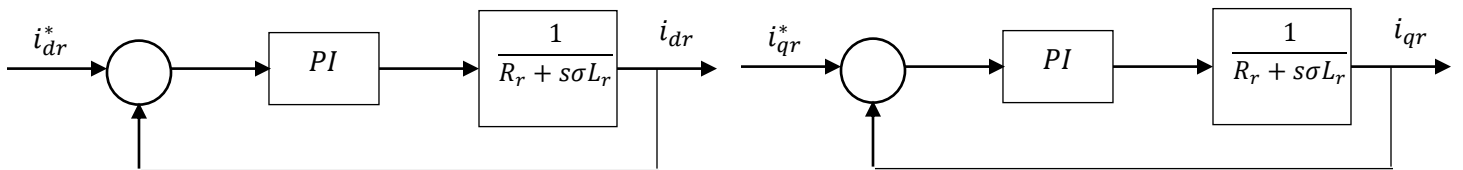Figure 7: Structure of grid side converter control

Figure 8: Rotor currents control block diagram

III. RESULTS AND DISCUSSION

MATLAB/Simulink environment was used to model and simulate a 2MW DFIG-based wind turbine Wind Energy Conversion system. The simulation was carried out with two different wind speeds and the performance of the machine was evaluated. The mechanical rotor speed is shown in figure 9. It can be seen that, at steady state, the speed changed from 142 rad/s to 146 rad/s corresponding to wind speed changes of 8 m/s and 10 m/s respectively. During simulation time, the DC link voltage is controlled to a constant value of 1150 V as shown in figure 10. The reactive power of the rotor is regulated to 0 VAR as shown in figure 11 as per the control strategy which ensures that no reactive power is exchanged with the grid. These results show the effectiveness of both the rotor and grid side controls. With a step increase in speed, there is increased grid current and hence increased rotor power at less torque according to the MPPT Algorithm. The corresponding rotor power and torque profiles are shown in figures 12 and 13 respectively. The constant DC bus voltage ensures that rotor power is constant as well at any wind speed operation.

At the speed of 10 m/s, the product of torque and speed can be seen to approach a value of 1.5 MW which is as predicted in figure 3. The grid current waveform is provided figure 14. It can be observed that it is a 50Hz, 3-phase sinusoidal current with amplitude of 500 A *pk-pk*. The system data is provided in table 1.
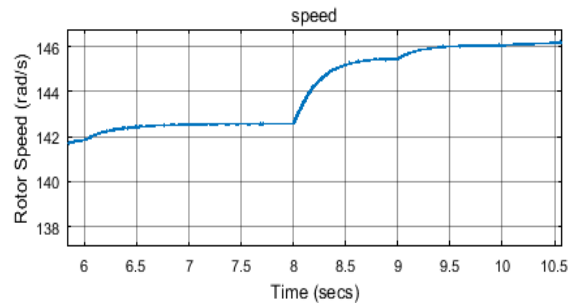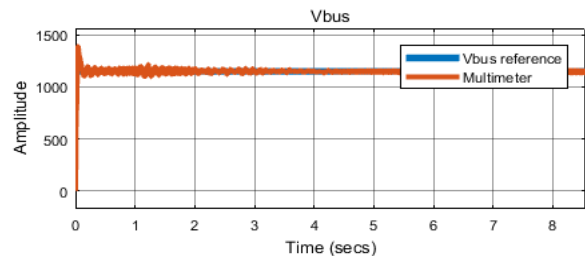

Figure 9: Rotor Speed
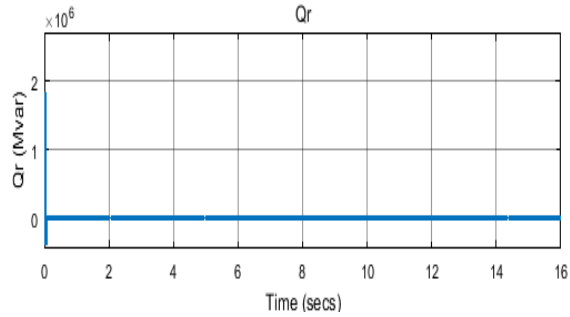

Figure 10: DC- bus Voltage
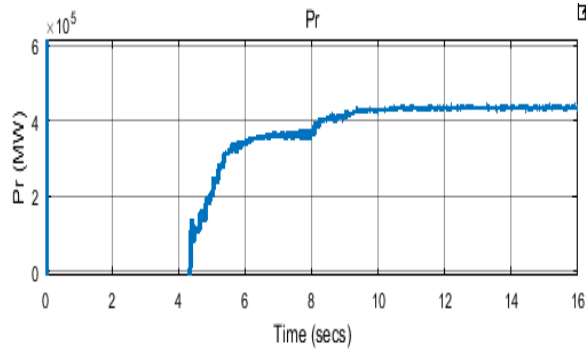
Figure 11: Rotor Reactive Power
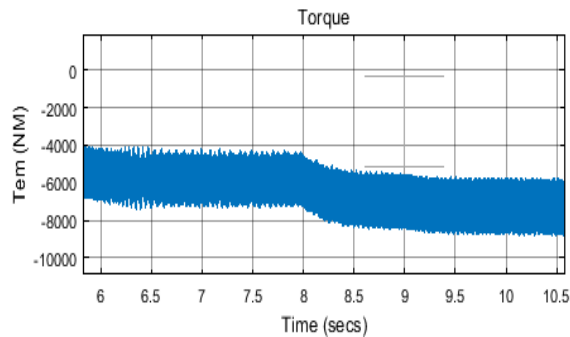

Figure 12: Rotor active Power
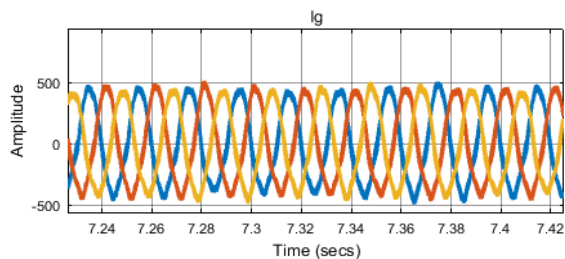

Figure 13: Torque Supplied

Figure 14: Grid Current

IV. CONCLUSION

This paper evaluated the performance of DFIG-based wind turbine in MATLAB/Simulink under two different wind speeds. The system model consists of the aerodynamic model of a three blade wind turbine, DFIG model, the model of the bidirectional converter

with its control. A clear procedure to obtain the proportional and integral controller gains for the current control loops was outlined. Simulation results show the effectiveness of both the rotor and grid side controls. Performance results were discussed with particular note that the DC link voltage was controlled to a constant value of 1150 V to keep rotor power constant while the reactive power of the rotor is regulated at 0 VAR to ensure that no reactive power is exchanged with the grid.

TABLE 1: DFIG PARAMETERS

PARAMETER	RATING
Rated Power	2MW
Stator/Rotor Turn Ratio	1/3
Rated Frequency	50Hz
Number of Pole	4
Stator Resistance	2.6mΩ
Rotor Resistance	2.9 mΩ
Stator Leakage Inductance	0.087mH
Rotor Leakage Inductance	0.087mH
Magnetism Inductance	2.5mH
Maximum Slip	1/3

REFERENCES

[1] Babu, B. C., & Mohanty, K. (2010). Doubly-fed induction generator for variable speed wind energy conversion systems-modeling & simulation. *International Journal of Computer and Electrical Engineering, 2*(1), 141.

[2] Sediki, H., Abdeslam, D. O., Otmane-cherif, T., Bechouche, A., & Mesbah, K. (2012). Steady-state analysis and control of double feed induction motor. *World Academy of Science, Engineering and Technology, 6*(1), 153-161.

[3] Yang, S.-Y., Wu, Y.-K., Lin, H.-J., & Lee, W.-J. (2014). Integrated mechanical and electrical DFIG wind turbine model development. IEEE Transactions on Industry Applications, *50*(3), 2090-2102.

[4] Chatterjee, D., & Hussain Rather, Z. (2018). Modelling and Control of DFIG-based Variable Speed Wind Turbine.

[5] Lavanya, N., Sekhar, O. C., & Ramamoorty, M. (2017). *Performance of indirect matrix converter with improved control feeding doubly fed induction machine.* Paper presented at the 2017 IEEE International Conference on Signal Processing, Informatics, Communication and Energy Systems.

[6] Amor, W. O., & Ghariani, M. (2014). *Modelling and Simulation for variable speed wind energy conversion systems based on doubly-fed induction generator.* Paper presented at the Electrical Sciences and Technologies in Maghreb (CISTEM).

[7] Abbas, F. A. R., & Abdulsada, M. A. (2010). Simulation of Wind-Turbine Speed Control byMATLAB. International Journal of Computer and Electrical Engineering, 2(5), 912.

[8] Khan, I., Zeb, K., Din, W. U., Islam, S. U., Ishfaq, M., Hussain, S., & Kim, H.-J. (2019). Dynamic modeling and robust controllers design for doubly fed induction generator-based wind turbines under unbalanced grid fault conditions. Energies, 12(3), 454.